

---

Article

# Non-invasive Probing of Winter Dormancy via Time-frequency Analysis of Induced Chlorophyll Fluorescence in Deciduous Plants as Exemplified by Apple (*Malus × domestica* Borkh.)

Boris Shurygin <sup>1,2\*</sup>, Ivan Konyukhov <sup>1</sup>, Sergei Khrushchev <sup>1</sup>, and Alexei Solovchenko <sup>1,2,3</sup>

<sup>1</sup> Faculty of Biology, Lomonosov Moscow State University, Leninskie Gory 1/12, 119234 Moscow, Russia

<sup>2</sup> Institute of Natural Sciences, Derzhavin Tambov State University, Tambov, Russia

<sup>3</sup> Federal Scientific Agroengineering Center VIM, Moscow, Russia

\* Correspondence: lodinn@lodinn.com; Tel.: +7(985)797-69-48

**Abstract:** Dormancy is a physiological state that confers winter hardiness to and orchestrates phenological phase progression in temperate perennial plants. Weather fluctuations caused by climate change increasingly disturb dormancy onset and release in many plant species including tree crops leading to aberrant growth, flowering, and fruiting. Currently, research in this field is impeded by the lack of affordable non-invasive methods for on-line monitoring of dormancy. We report on an automatic framework for low-cost, long-term, and scalable dormancy studies in deciduous plants. The proposed method is based on continuous near-field sensing of the photosynthetic activity of shoots via pulse-amplitude modulated chlorophyll fluorescence sensors connected remotely to a data processing system. The resulting high-resolution time series of JIP-test parameters indicative of the responsiveness of the photosynthetic apparatus to environmental stimuli are subjected to frequency-domain analysis. The proposed approach allows to overcome the variance coming from diurnal changes of insolation and to derive estimations on the depth of dormancy. Our approach was validated over three seasons in an experimental apple (*Malus × domestica* Borkh.) orchard by collating the non-invasive estimations with the results of traditional methods (growing of the cuttings obtained from the tress at different phases of dormancy) and the output of commonly used chilling requirement models. We discuss the advantages of the proposed monitoring framework such as prompt detection of freeze damages along with its potential limitations.

**Keywords:** chilling requirement; chlorophyll fluorescence; non-photochemical quenching; PAM; photoprotection; stress resilience; winter dormancy

---

## 1. Introduction

Winter dormancy is a physiological state characterized by physiological quiescence and hence by increased resilience to harsh environmental conditions such as low temperatures. It is among the key adaptations of perennial plant species, including temperate annual and deciduous plants, for survival during the cold season [1] (pp. 309-314).

Winter dormancy proceeds through the three phases: the first phase is pre-dormancy, during which mechanisms increasing stress tolerance of plants are deployed [2]. It is followed by physiological or deep dormancy, endo-dormancy [3,4]. Endodormancy is defined as inactive state of meristems and/or organs capable of growth in which growth does not resume even under favorable conditions until this state is changed by environmental signals [5,6]. The onset and release of dormancy is synchronized with seasonal climate changes; as noted above, it ensures preservation of shoot tissues, vegetative and generative buds during the cold season [7,8].

Upon exposure to low temperatures during the cold season, plants progress from endo-dormancy to the next phase—eco-dormancy—when growth is restricted only by unfavorable climatic conditions; this event is called dormancy release [2,4]. Although the

mechanisms of the dormancy onset, maintenance, and release are still being debated, these phenomena are believed to be jointly controlled by the expression of certain genes, hormonal balance, and environmental stimuli such as temperature and photoperiod [9-12]. Thus, the release of endo-dormancy requires exposure to low temperatures termed as chilling requirement (CR), which is expressed in chilling units (CUs) and reflects the amount of plant exposure at low temperatures, most commonly in the range of 0–7 °C. The CR varies depending on genotype and regional climate [13,14]; it can be predicted using several mathematical models (see [15] and references therein).

Increasing research interest in winter dormancy is also fueled by its practical importance for crop production, especially for growing fruits in regions with unstable climatic conditions. The problem of insufficient chilling exposure has become especially urgent in recent years [8,16]. Weather fluctuations causing aberrant dormancy onset or its premature release impair stress resilience of plants making them vulnerable to frost snaps common in the beginning of the vegetation season, and deteriorate floral bud formation and fruit set. These effects are already being observed in warm winter regions [16,17]. Therefore, researchers and breeders need estimations of dormancy depth for plant phenotyping and breeding for hardiness. Determination of the CR and corresponding growing zones for a given cultivar are high priority tasks for agricultural sustainability and food security, but they can hardly be performed at scale because of the destructive nature of the dormancy assessment. Despite the importance of the problem, only a limited set of methods is available for studies of dormancy. Both conventional (growing of the cuttings taken from plants at different phases of dormancy) and recently developed methods (e.g., those gauging the expression of dormancy-related genes [11,18] are invasive. To overcome this limitation, a technique for on-line assessment of dormancy state is desirable.

A plausible approach compatible with these requirements is based on recording and analyzing the amplitude-kinetic characteristics of pulse-amplitude modulated (PAM) induced chlorophyll fluorescence (CF) widely used in high-performance plant phenotyping [19-21]. In this approach, chlorophyll *a* serves as an "internal probe" of the photosynthetic apparatus (PSA) condition reflecting indirectly the metabolic activity of tissues hence it is expected to reveal inter alia the dormancy status of plants.

The CF/PAM-based techniques became widespread in the past decades as a promising approach to vegetation sensing giving deep insights into various aspects of physiological condition of plants and their stress resilience [22-24]. Thus, a CF/PAM-based protocol was developed for assessment of winter hardiness [25] and dormancy of conifers [26], but it did not allow for separating the effects of low temperature and those of solar radiation intensity. In deciduous plants including tree crops, CF induction curves can be recorded directly from the shoots whose phelloderm contains chloroplasts capable of photosynthesis [27-30] so that the CF/PAM-based approach turned to be applicable to deciduous plants throughout the cold season [25], but it was never automated and did not allow time-resolved measurements so far.

In *Fagus sylvatica*, leaves and shoots demonstrated the same pattern of Fv/Fm changes in the spring-summer period [30]. It was also shown that CF of the shoots was related to the cold resistance of willow clones and the degree of frost damage to their cambium [31]. Current evidence suggests that the temperature dependence of the CF parameters can be, in principle, used as a proxy for identifying cold-resistant plants. Still, CF-based approaches capable of resolving the onset and release of winter dormancy (endo-dormancy) are so far lacking. Winter hardiness of dormant conifer plants was associated with the induction of a high, slowly relaxing NPQ dependent on phosphorylation of thylakoid proteins and up-regulation of the violaxanthin cycle [32-34]. Another luminescent marker of dormancy is thermoluminescence: its B-band declines at early stages of in pine needle hardening, likely due to increased charge recombination in PS II providing additional photoprotection [35]. Taken together, the published reports available to the authors of this work do not present a conclusive approach to non-invasive assessment of winter dormancy via CF induction curves, especially that suitable for deciduous trees. At the same time, new and upcoming climate challenges result in an increased demand for

an affordable, scalable, and non-invasive approach to dormancy monitoring from researchers, breeders and growers alike.

Here, we report on a novel approach to record and treat CF data for non-invasive online assessment of dormancy depth of and frost damage to trees exemplified by apple. It assumes that physiological and biochemical rearrangements accompanying the onset and release of dormancy in plants also trigger measurable changes in the functioning of the photosynthetic apparatus (PSA). In turn, these changes are reflected in the long-term dynamic of the CF/PAM parameters known as JIP-test [22,36-38] which are further subjected to time-frequency analysis.

## 2. Results and discussion

To find an approach to selective and sensitive non-invasive monitoring of the onset and release of winter dormancy in the model deciduous plants, a long record of CF/PAM and weather data obtained across seasons over several years was studied. Resultant periods of conjectured endo- and eco-dormancy were validated against traditional criteria of dormancy and the corresponding arrays of non-invasively recorded data were subjected to multi-step mathematical analysis to reveal parameters potentially indicative of the dormancy depth.

### 2.1. Winter dormancy and dormancy release

According to multi-year observations, in the growing region where our experimental plot is situated, the onset of winter dormancy in apple trees normally starts at September-October and completes by mid-November. The release of endo-dormancy and transition to eco-dormancy occur, depending on the specific season conditions, from the end of January till mid-February.

To establish the objective reference for the non-invasively obtained data, we have tested the depth of dormancy using a traditional destructive test—growing of the cut-off shoots under the room conditions (see Materials and Methods, Figure 8). Since it was not possible to cut shoots frequently from the experimental trees due to their young age, the destructive tests were used only to validate the key phases of dormancy (eco-dormancy and endo-dormancy) in each season. Under our experimental conditions, the shoots collected in late November remained dormant (no budbreak was observed). By contrast, the shoots sampled in the middle of February displayed budbreak and subsequent growth of leaves and, in many cases, developed flowers within 10–14 days. Overall, the results of the destructive tests carried out in this work were in line with the multi-year observation on the onset and release of winter dormancy in apple trees in the location where the experimental orchard was planted. An exception was observed in the season 2020 featuring a warm winter (average temperature in November–December was above  $-5^{\circ}\text{C}$ ), when the dormancy progression was highly erratic. The time points corresponding to the sampling of shoots displaying the absence or presence of budbreak under favorable conditions are marked on the figures below.

### 2.2. Chlorophyll fluorescence transients

The work was started by pilot experiments on comparison of the OJIP transients taken from the shoots incubated at different temperatures:  $-18^{\circ}\text{C}$  (a common winter temperature at the site of the experimental orchard), warmed up to  $25^{\circ}\text{C}$ , and frozen at liquid nitrogen temperature (around  $-195^{\circ}\text{C}$ ). The OJIP curves recorded  $-18^{\circ}\text{C}$  and  $25^{\circ}\text{C}$  (Figure 1, curves 1 and 2) were similar and contained the features characteristic of the PSA of healthy plants (for more details, see e.g. [37]). At the same time, the OJIP curves of the shoots kept at  $-18^{\circ}\text{C}$  were characterized by a lower overall amplitude resulting in a lower  $F_v/F_m$ .

The OJIP curves of the shoots incubated in liquid nitrogen (LN) were dramatically different in their shape from those taken from the intact shoots (cf. curves 1, 2 and 3, 4 in Figure 1). Notably, the shape of the LN-frozen curves did not change significantly after

thawing the LN-frozen shoots. Obviously, the observed changes reflect the destruction of the PSA and, ultimately, death of the shoot tissues. The latter conclusion was supported by the absence of budbreak, and growth of the LN-frozen shoots further incubated at 25 °C.

Overall, the healthy cold-acclimated apple tree shoots exhibited measurable CF transients with characteristic features of viable plant tissues. On the contrary, irreversible frost damage has changed the shape of chlorophyll fluorescence transient dramatically. Accordingly, our pilot measurements showed the feasibility of the recording of OJIP curves from sound apple shoots at cold season. As an added benefit, analysis of the OJIP curves turned to be capable of rapid on-line detection of frost damage without the need of laborious laboratory tests and observations.

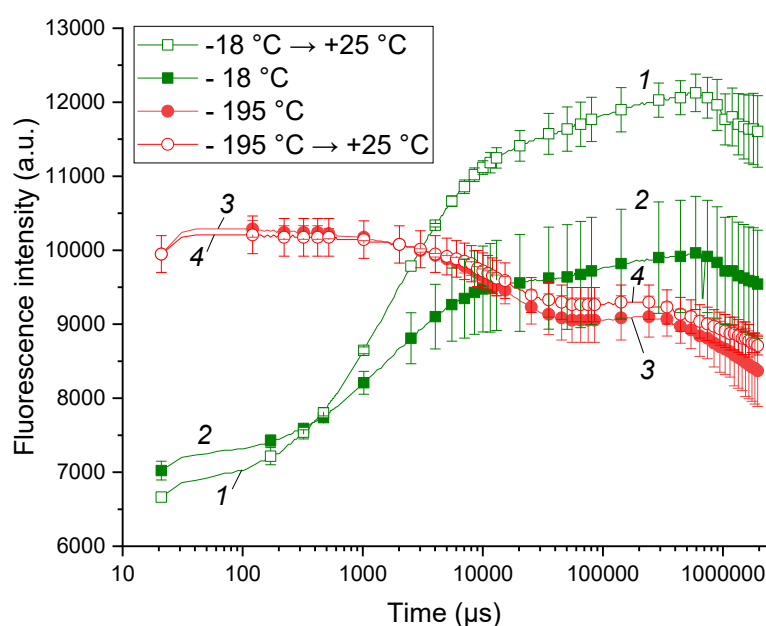


**Figure 1.** Difference between the chlorophyll a fluorescence induction curves of live apple tree shoots (1, 2) and those irreversibly damaged by liquid nitrogen freezing (3, 4). Typical OJIP curves of the apple tree shoots maintained at  $-18\text{ }^{\circ}\text{C}$  (2) and subsequently warmed up to  $25\text{ }^{\circ}\text{C}$  (1) as well the OJIP curves of the apple tree shoots frozen in liquid nitrogen ( $-195\text{ }^{\circ}\text{C}$ ; 3) and subsequently warmed up to  $25\text{ }^{\circ}\text{C}$  (4).

### 2.3. Long-term correlations of the CF parameters and weather conditions

To monitor the CF transients directly from the shoots of the trees planted in the orchard, the custom-made PAM sensors (Figures S1, S2) were made capable of wireless transmitting of hourly measured OJIP curves to a remote server for processing and visualization and the examples of raw CF transients (Figures S3, S4). In total, over 35000 transients and over 16000 weather measurements were collected and processed over the observation period. To establish candidate parameters for further analysis, a set of correlation matrices was produced for the complete dataset (Figure 2) as well as for the data obtained around midnight (Figure S6) or midday (i.e. under the highest sunlight intensity, Figure S5).

Of all meteorological parameters monitored, only air temperature strongly correlated with the condition of PSII (e.g.,  $r[\text{Fv}/\text{Fm vs. air } t^{\circ}] = 0.75$ ). Certain JIP test parameters included in the initial dataset were, by definition, inter-correlated and hence redundant. These parameters are not shown in the figure, but could be found in plots in supplementary materials, as well as plots of Spearman's rank correlation, which were found to differ

insignificantly from Pearson's  $r$  values. Still, the analysis of correlation coefficients calculated for the complete dataset across seasons and years (designated as "bulk correlations" here) yielded several useful hints. Thus, maximal quantum yield of photosystem II (PS II),  $F_v/F_m$  (see Table S1), the parameter by far the most frequently used as an integral indicator of physiological condition of plant organism [39], has shown a strong correlation with air temperature (Figure S6) but not with other weather parameters indicating a sizeable influence of this factor on the performance of the PSA.

Surprisingly, the correlation of the studied parameters with the flux of thermally dissipated energy ( $DI_0/RC$ ) was low (Figure 2). All JIP-test parameters studied demonstrated a weak correlation with UV radiation intensity and calculated total solar radiation fluxes. Collectively, the results of the "bulk correlation" analysis suggested that the air temperature exerted a more profound effect on the condition of PSA of the trees during their winter dormancy as compared with light intensity. At the same time, the  $r$ -values for these correlations were generally low.

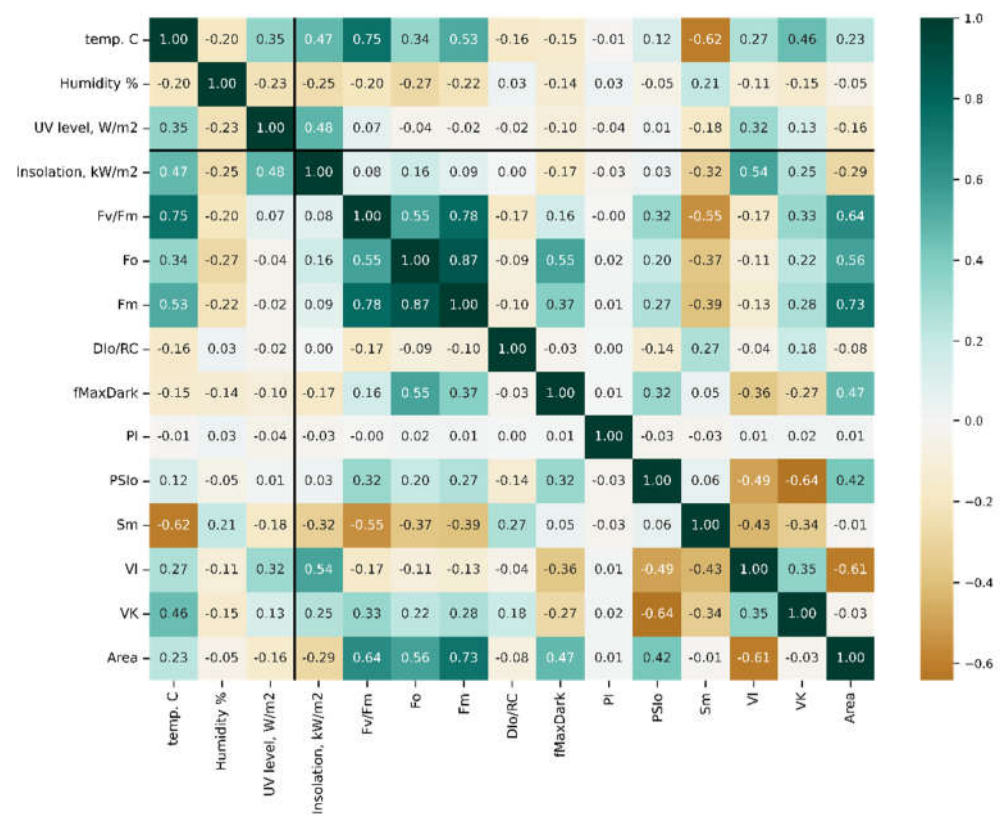


**Figure 2.** Pearson's  $r$  value matrix computed for pairs of the parameters studied in this work. Thick lines delineate fluorometry from meteorological data. For more detail on JIP test parameters, see also [40], Table S1, and Figures S5, S6.

Since the selectivity and sensitivity of the "bulk correlation" analysis was rather limited, we have had a closer look at monthly average values of the JIP-test parameters. Most of the parameters analyzed displayed a high variation and a lack of conclusive trend (not shown). A spectacular exception was constituted by the  $F_v/F_m$  and  $DI_0/RC$  parameters (Figure 3). Thus, dark-adapted (measured at night) values of  $F_v/F_m$  tended to decline during the onset of endo-dormancy and increased when the dormancy was released; light-adapted values have demonstrated an opposite trend (Figure 3a).

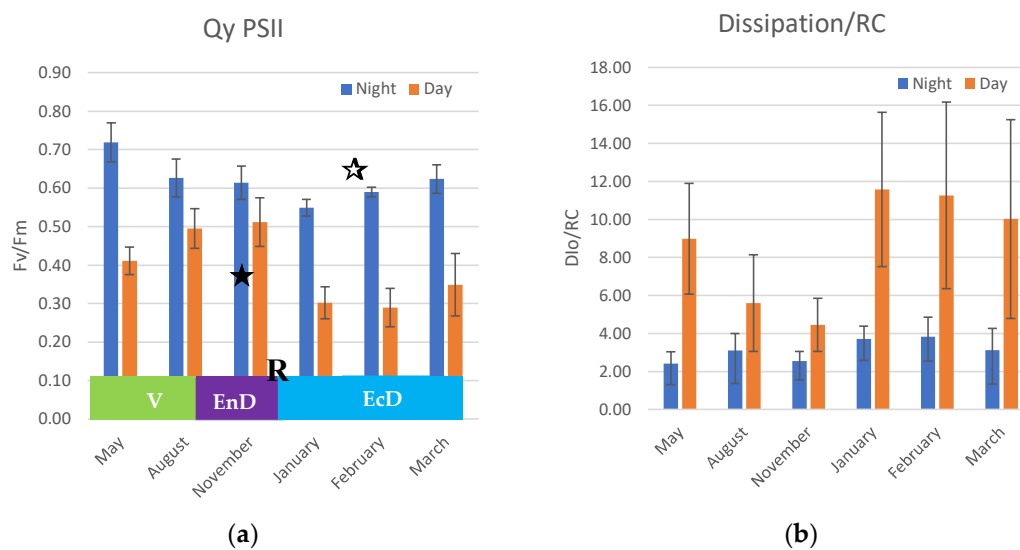


**Figure 3.** Monthly average values of (a) photosystem II quantum yield; (b) thermal dissipation per reaction center calculated at midnight and midday values (indicated on the graphs) during active vegetation (May), onset (August-November), maintenance (January), and release (February-March) of endo-dormancy. The annotations in the bottom denote approximate duration of dormancy and vegetation phases (V, vegetation period; EnD, endodormancy; EcD, ecodormancy; R, endodormancy release; destructive tests: ★, no budbreak displayed by the cut shoots; ☆, budbreak in room conditions).

In the case of  $DI_0/RC$  measured under daylight conditions (Figure 3b), there was a pronounced decline during the onset of endo-dormancy followed by a sharp increase in this parameter when the dormancy was released. Notably, the magnitude of changes in  $DI_0/RC$  was much higher than in  $F_v/F_m$  (3-fold vs. around 1.5-fold, respectively). Nighttime values of this parameter, as expected, did not show a clearly visible trend of changes.

In view of the findings outlined above, we hypothesized that the depth of winter dormancy in the studied plant object should be somehow related with responsiveness of the photoprotective responses to the PSA to harsh environmental conditions. Accordingly,  $F_v/F_m$  and  $DI_0/RC$  were selected as candidate parameters for further analysis on the grounds of their high dynamic range and relatively low noise. On one hand, the engagement of the photoprotective mechanisms depends on the incident PAR flux and the presence of other stresses such as low air temperature. On the other hand, we did not see a pronounced difference in the correlations between the parameters measured at daylight and at night. Therefore, we attempted to deconvolute the time-frequency behavior of the kinetics of  $F_v/F_m$  and  $DI_0/RC$  using the time-resolved data recorded hourly across seasons (see Materials and Methods).

#### 2.4. Time-frequency analysis of the CF data

For purposes of forward analysis, an attempt was made to predict  $F_v/F_m$  solely from recorded temperatures and insolation estimates (see Materials and Methods, Equation 2). While the resulting approximation displays a significant amount of inter-dependency between parameters, such a simple model could not capture complex relations and overestimated the effects of temperature (Figure S8). Yet, at  $r^2 = 0.68$ , the goodness of fit is remarkably high as compared to that for  $DI_0/RC$  (at just  $r^2 = 0.07$ ) – the fraction of explained variance interpretation thus suggests  $F_v/F_m$  being highly volatile. That is,  $F_v/F_m$  appears to be affected to a high degree by the transient, high-frequency environmental changes – specifically, changes in insolation and temperature. Conversely,  $DI_0/RC$  remains largely unaffected by those outside of eco-dormancy, which is further corroborated by the analysis below.

Autocorrelation plots (Figure S7) have demonstrated remarkably strong daily periodicity of Fv/Fm, but vanishingly small day-to-day consistency for parameters reflecting fluxes of energy per reaction center such as  $DI_0/RC$ ,  $ET_0/RC$ ,  $TR_0/RC$ . In *P. silvestris* and *Picea abies*, despite significant differences in their mechanisms of acclimation to low temperature, Fv/Fm follows the time-course of ambient temperature [41]. In *P. silvestris*, a decline in Fv/Fm can be used to predict cold resistance [42]. Thus, for late-flowering almond (*Prunus dulcis*) varieties with pronounced susceptibility to frost, a linear decrease in Fv/Fm with temperature was found, and for early-flowering varieties of the same species resistant to low temperatures, a quadratic curve with an inflection point at  $-1$  °C was observed [43]. However, the actual (operational) quantum output of PS II is more sensitive than Fv/Fm, because it can change rapidly [44], while a decrease in Fv/Fm can be detected only at the deep stages of hardening or winter stress [45].

Under our experimental conditions, the parameters expressed on RC basis were more informative with respect to the transition throughout phenological stages and stable downregulation of PSII activity. Indeed, earlier research highlighted the intimate connection between chilling and photoinhibition, which is especially pronounced in apple trees (see [46] and references therein).

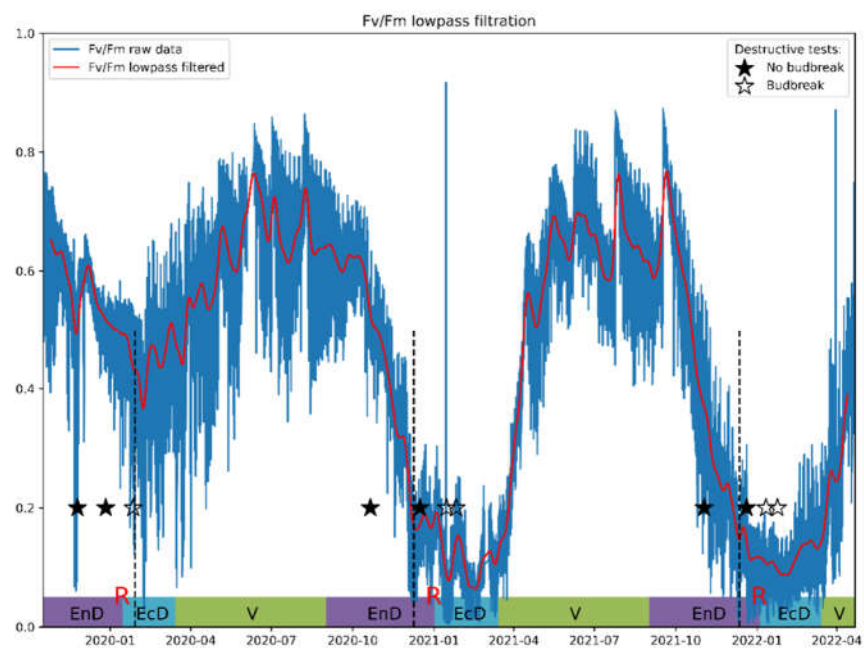


**Figure 4.** A typical view of an actual Fv/Fm record and its general trend obtained by the lowpass filtering of the respective time series. For meaning of the annotations, see the legend to Figure 2.

Low-pass filtering was found to produce relatively smooth resulting curves starting from the filter transition width corresponding to one week (Figure 4). The frequency response of the filter and results for other JIP test parameters can be found in supplementary materials. After filtration, these curves reveal that Fv/Fm *per se* is a sensitive, but not sufficiently selective indicator of cold acclimation and dormancy, which are known to go hand in hand in apple [47]. Thus, during the unusually warm winter of 2019/2020, Fv/Fm has hardly dipped below the values typical of vegetation season.

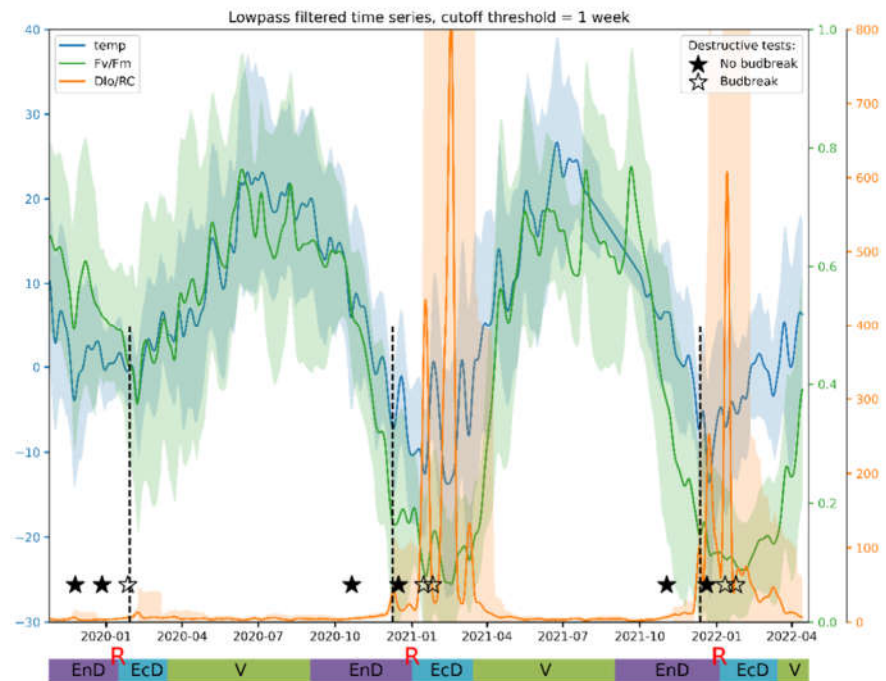


**Figure 5.** The time-courses of air temperature and the spectral power of the PS II  $Q_y$  ( $F_v/F_m$ ) and thermally dissipated energy flux ( $DI_0/RC$ ) variations with the period of one week (lowpass filtered value  $\pm 2 * STD$ ). The plots and the corresponding Y-axis are drawn in same color. Annotations: V, vegetation period; EnD, endodormancy; EcD, ecodormancy; R + vertical dashed line, endodormancy release. Destructive tests: ★, no budbreak displayed by the cut shoots; ☆, budbreak in room conditions.

The  $DI_0/RC$  parameter exhibits a similar trend of change, but the fine structure of its broad winter peak is much more pronounced and easier to study numerically (Figure 5). Of special interest is the period corresponding the winter of 2020–2021, which was mild with average temperatures around  $-1$  °C. Under such conditions, the increase of  $DI_0/RC$  is barely detectable as compared to frosty winters of two subsequent seasons (Figure 5, see also Figure 6b below). The dormancy release in the season 2020–2021 was also delayed by at least three weeks.

Wavelet analysis carried out as described in Materials and Methods (see also the Theoretical background subsection in Supplementary) confirmed the hypothesis that  $DI_0/RC$  conveys more information about the dormancy depth in apple than  $F_v/F_m$ .  $F_v/F_m$  spectrogram shows (Figure 6a) a separation between daily cycles (top horizontal black line, bottom black line corresponds to a period of one week) and slower changes owing principally to weather conditions. The general trend of changes in spectral power (which is assumed reflective of the magnitude of relative contribution of the processes and/or stimuli with corresponding frequency of oscillation) is hard to uncover, and the spectrogram is noisy overall indicating many processes affecting  $F_v/F_m$  are happening at once. Whereas  $F_v/F_m$  could be used to trace general trends in data, it is not selective enough to describe changes specific to certain phase of dormancy.

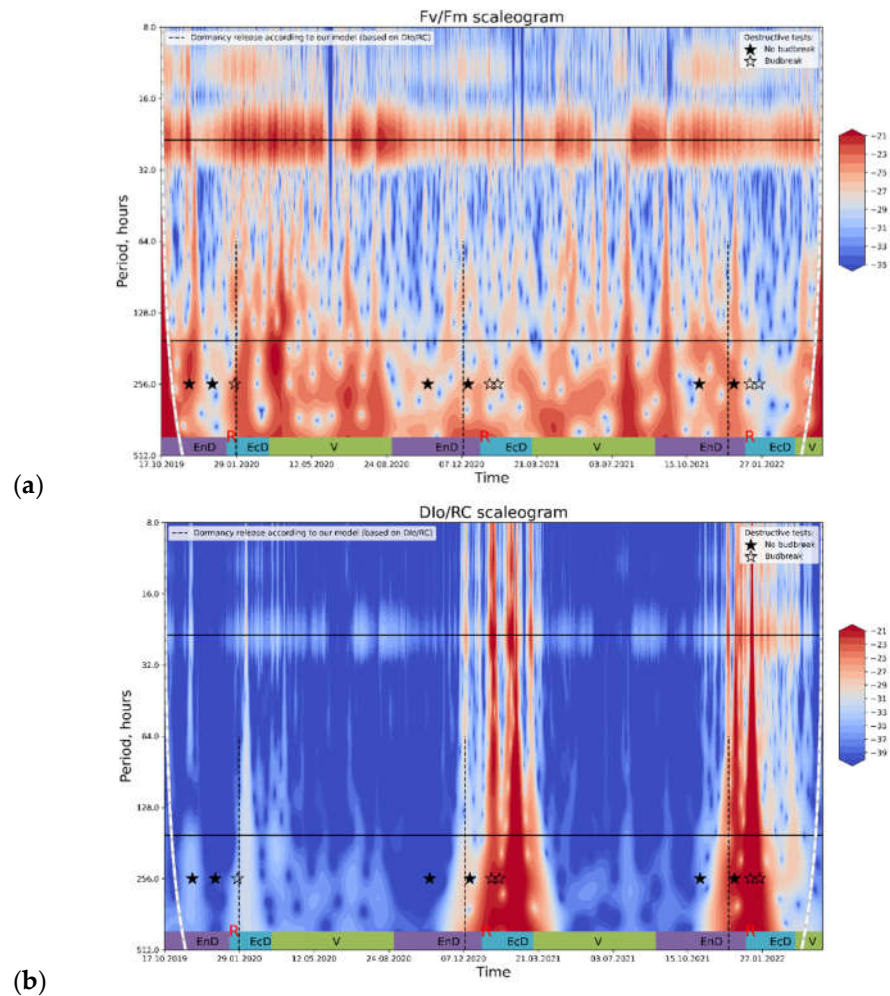


**Figure 6.** The results of wavelet transform analysis of (a) PS II Qy; (b) thermally dissipated energy flux per reaction center. An increase in spectral power pertinent to the processes influencing the OJIP parameter in question (red-colored regions on the plot) is tentatively ascribed to the periods of end-dormancy release and the onset of eco-dormancy. For explanations, see text. Annotations: V, vegetation period; EndD, endodormancy; EcD, ecodormancy; R + vertical dashed line, endodormancy release. Destructive tests: ★, no budbreak displayed by the cut shoots; ☆, budbreak in room conditions.

By contrast, DI<sub>0</sub>/RC spectrogram (Figure 6b) shows clear peaks corresponding to eco-dormancy phases, a similar pattern is evident on the plots with the results of low-pass filtration of the DI<sub>0</sub>/RC signal (Figure 5). Importantly, the prominent peaks of spectral power evident on both types of plots corresponded to the periods of time when dormancy was already released and eco-dormancy took place, according to the destructive tests with the cut shoots.

Although both Fv/Fm and DI<sub>0</sub>/RC reveal valuable information about the physiological condition of plant, all of the analysis performed supports the conclusion that the dormancy in woody plants is better described in terms of the oscillation of photoprotective thermal dissipation in response to the cold and high sunlight stresses rather than by quantum yield of PS II. DI<sub>0</sub>/RC also holds promise as a measurable marker of the mechanisms driving the metabolic changes during dormancy, whereas Fv/Fm is an integral characteristic not specific to any single type of stress. While Fv/Fm is better suited for the overall assessment of the PSII state, we suggest the kinetics DI<sub>0</sub>/RC and other per-RC characteristics as candidates for the research on cyclic processes with relatively long periods (on the scale of weeks and months).

### 2.5. Agreement of the non-invasive dormancy assessments to those derived from the common CR mathematical models

To further validate our conclusions regarding the applicability of the proposed approach, we confronted our assessments of dormancy status of the experimental plants with predictions yielded by the most widespread mathematical models [15]: the model based on chilling hours [48], the Utah model [49], and the “Low chill” model [50], and North Carolina model [51] from the weather information collected during the observation period. The predictions of the periods when eco-dormancy release was expected were in reasonable agreement with the assessments made on the basis of the time series analysis (Figure 7) further supporting the validity of the approach developed here.

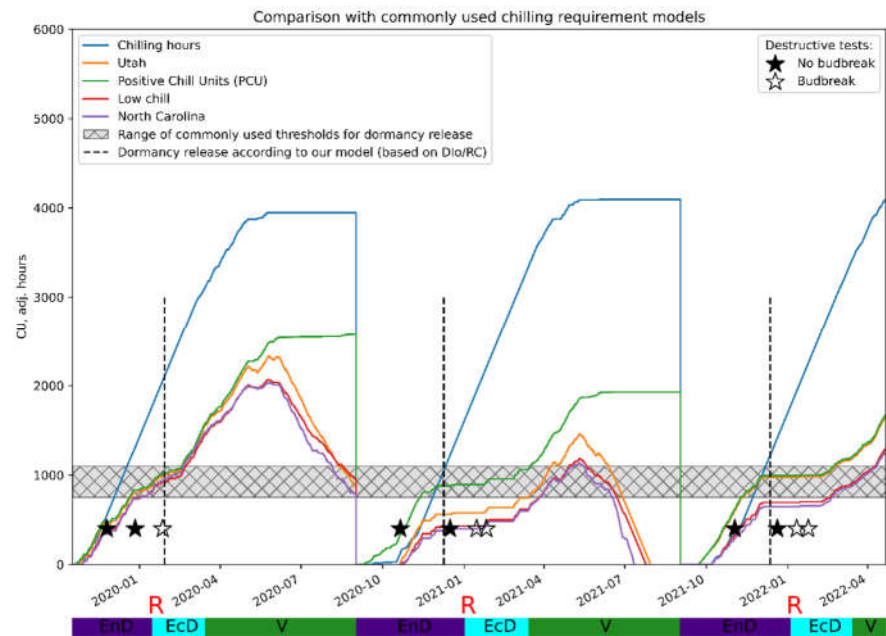


**Figure 7.** Comparison of the predictions of the endo-dormancy obtained using the wavelet analysis of the  $DI_0/RC$  time series (see Figures. 4 and 5) and those inferred from the established CR models (see Materials and Methods). The vertical dashed lines denote the transition from endo-dormancy to eco-dormancy.

### 3. Materials and Methods

#### 3.1. Plant material and experiment design

The experiments were carried out at an experimental orchard located in the Botanical Garden of Lomonosov Moscow State University (55.7078 °N, 37.5268 °E) using three-year old apple (*Malus × domestica* Borkh.) var. “Flagman” plants grafted on B-396 rootstock planted according to the 2.5× 0.8 scheme and trained as “spindle”. The experiment has been carried out throughout October 2019–May 2022.

To confirm the onset of endo-dormancy indicated by the online non-invasive measurements (see below), five 20-cm shoots were cut from the experimental trees several times in the end of November–beginning of December and grown in tap water under room conditions. To confirm the release of endo-dormancy, the same number of shoots was cut in the end of January–mid-February and grown under the same conditions. The absence of budbreak within 10-day period was considered a confirmation of the onset of endodormancy whereas budbreak, growth and development of leaflets and flowers (Figure 8) have been accepted as a confirmation of dormancy release.



**Figure 8.** Release of endodormancy: (a) budbreak and (b) flowering of the apple tree shoots collected in February 2021 and grown in tap water at room temperature.

The frost damage simulation experiments were conducted after release of endo-dormancy (February 2019). The shoots were cut at the orchard at 10:00 a.m. and kept at  $-18\text{ }^{\circ}\text{C}$  in darkness. For the five control samples, OJIP curves were recorded (i) at  $-18\text{ }^{\circ}\text{C}$  and (ii) after warming them up to  $+25\text{ }^{\circ}\text{C}$  in darkness. For the other five shoots, OJIP curves were recorded at  $-18\text{ }^{\circ}\text{C}$ , then the shoots were dark-frozen in liquid nitrogen ( $-195\text{ }^{\circ}\text{C}$ ) for 30 min. The OJIP curves were then recorded from the frozen shoots after warming them up to  $+25\text{ }^{\circ}\text{C}$ , also in darkness.

#### 3.2. Chlorophyll fluorescence and weather data collection

For recording Chl fluorescence induction curves of the shoots incubated indoors, FluorPen S100 (Photon Systems Instruments, Drasov, Czech Republic) and its built-in “OJIP” protocol was used. For continuous outdoor measurements, two in-house made

PAM-fluorometers were fixed on the internodes of 2-year shoot (around 1.5 cm in diameter) in the middle part (ca. 1.5 m above ground) of the canopy of two different apple trees (Figures 9a, b). The PAM sensors employed the Fast-Repetition-Rate technology, FRR [52] and possessed the same characteristics as the earlier developed devices [53], for more detailed information, see the description of the device in the supplementary materials including Figures S1, S2.

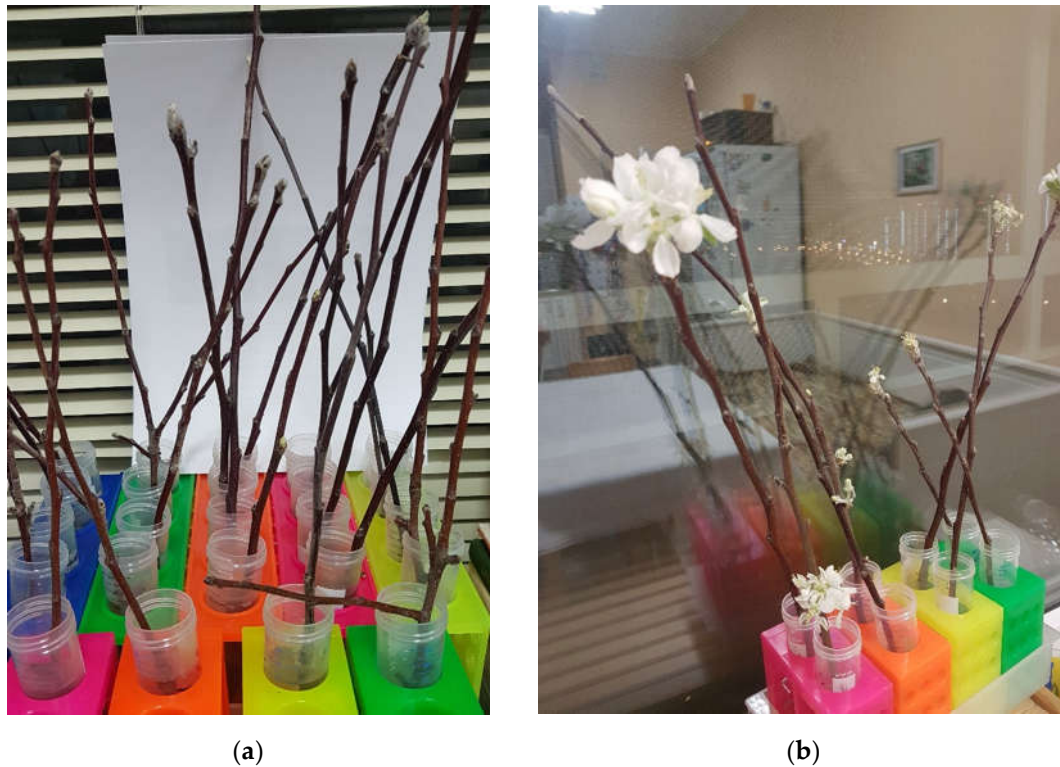


**Figure 9.** Sensors of variable chlorophyll fluorescence mounted on the monitored trees in the experimental orchard of Lomonosov Moscow State University in (a) fall and (b) winter seasons along with (c) a representative screenshot with hourly logged values of the OJIP parameters.

The experiment has been started with a single PAM fluorometer (19 October 2019–6 February, 2020), after that, a second unit was added for redundancy and cross-validation. Once an hour, each PAM sensor transmitted the measured fluorescence transients (OJIP-curves) to an in-house developed remote server for archiving, processing (see below), and

visualization (Figure 9c). An automatic weather station (Sokol-M, GSK Escort, Kazan, Russia) was remotely connected to the same server to complement the CF/PAM data with current weather parameters (air temperature, relative humidity, atmospheric pressure, precipitation, wind strength and direction, as well as solar UV intensity).

### 3.3. Analysis of fluorescence transients (JIP-test)

Raw fluorescence transients were routinely processed using the pyPhotoSyn software [54] to calculate JIP-test parameters according to Strasser et al. [40]. Minimal fluorescence  $F_0$  and initial slope of the fluorescence transient  $M_0$  were estimated as the intercept and the slope of linear approximation of the initial linear segment of the fluorescence transient according to Plyusnina et al. [55]. For the complete list of JIP-test parameters, see Supplementary Table S1.

### 3.4. Data processing and analysis

Further processing was done in Python (version 3.8). First, the weather data was interpolated to the grid defined by the PAM fluorometers timestamps. Parameters derived from the JIP test were cleaned up, with values of far-flung outliers set to zero at the first stage of processing. Negative values and values exceeding the normal range more than tenfold were filtered out that way.

After that, exploratory data analysis was performed: JIP-test parameters were subjected to cross-correlation and auto-correlation analysis. To estimate the apparent dependence of the parameters on transient environmental conditions, multiple linear regression was used. This qualitative reconstruction of the parameter dynamics from insolation and temperature was then considered an indirect measure of how much information a given parameter provides about short-term vs. long-term plant adaptation. Finally, time-frequency analysis of the PSII characteristics as revealed by JIP-test was performed.

For modeling purposes, the entire dataset was augmented by solar elevation angles with the help of skyfield package using DE431 ephemeris [56]; these angles follow directly from the location, date and time of the measurement and provide an estimate of insolation. Potentially available sunlight was approximated by the formula

$$I_D = 1.353 \cdot 0.7^{(AM^{0.678})}, \quad AM = 1/\cos(\theta), \quad (1)$$

where  $AM$  is air mass,  $\theta$  is the solar zenith angle (complementary to the solar elevation angle), and  $I_D$  is the direct component of insolation (in  $\text{kW m}^{-2}$ ) [57]. The parameters yielded by JIP-test were then fitted by a multi-linear function of temperature and direct sunlight:

$$X = k_1 + k_2 \cdot T + k_3 \cdot I, \quad (1)$$

where  $T$  is temperature (in degrees Celsius) and  $I$  is insolation (in  $\text{kW} \cdot \text{m}^{-2}$ ). This model is intentionally simplistic and does not take into account cumulative effects of exposure to low temperatures and sunlight; it allows for the goodness of fit to be used as a metric. Here, the higher  $r$ -squared for modelling a given parameter is, the more this parameter is affected by transient changes and less it could reveal about the long-term dormancy-related changes.

Time-frequency analysis was performed on a subset of parameters chosen using correlation analysis (both Pearson's  $r$  and Spearman's  $\rho$  were calculated to capture both linear and non-linear relationships) and multi-linear regression models described above. Auto-correlation curves were also produced for estimating periodicity in signals as an indirect measure of dependence of a given parameter on changes in insolation and temperature driven by daily cycles. Spectrograms were produced using the pycwt package using a Morlet mother wavelet with the default value of  $w_0 = 6$  and frequencies corresponding to the range of one hour to 512 hours. Low-pass filtering using Fourier transform and the cutoff frequency of (one week) $^{-1}$  was also performed.

Relevant code used in the analysis is available on GitHub (<https://github.com/Lodinn/PAM-timeseries>).

To infer predictions of the CR accumulation sufficient for dormancy release, we employed the most widespread mathematical models [15]: the «chilling hours» model (Weinberger, 1950 [48]), the «Utah» model (Richardson et al., 1974 [49]), the «Low chill» (Gillreath and Buchanan, 1981 [50]), and the «North Carolina» models (Shaltout and Unrath, 1983 [51]).

#### 4. Concluding remarks

Dormancy is a complex phenomenon controlled by superposition of environmental stimuli (chiefly by photoperiod and temperature), mechanisms of perception and transmission of these signals, as well as the plant's responses to them. Our understanding of the mechanisms of the induction and regulation of winter dormancy and its phenotypic manifestations at the level of PSA is clearly insufficient. To overcome this limitation, we attempted to develop an approach to non-invasive express assessment of the winter dormancy depth in deciduous plants via CF induction curves using apple trees as a model. This problem has been tackled previously [25,42], but the previous attempts assessed, directly or indirectly, a magnitude of photoprotective response of PSA to the combined action of low air temperature and sunlight. Although CF is a sensitive probe of plant condition, it is easily affected e.g., by variations in ambient illumination conditions. Furthermore, acclimation to diverse factors such as cold and light intensity converges on PSA functioning [58,59] interfering with the manifestation of intrinsic processes like the onset release of endo-dormancy. Indeed, a significant complication of the non-invasive approaches is constituted by the need to disentangle the effects of diverse environmental stimuli and intrinsic responses connected by a complex web of regulatory mechanisms. Long-term (seasonal) trends e.g., those associated with dormancy are obscured by short-term responses to weather fluctuations profoundly affecting plant metabolic status and PSA functioning.

Overall, the variability of external stimuli and plant adaptation capabilities was large enough so the individual measurements of CF-based parameters turned to be unsuitable for assessing the dormancy depth. Indeed, the same value of any given parameter could be bearing vastly different implications depending on weather patterns. However, time series collection and analysis have a potential to reveal the seasonal long-frequency response over the background of stochastic acclimatory changes occurring on the timescale of days and hours.

In this work, we made a step towards extracting useful information on winter dormancy from detailed time series of JIP-test parameters. Only a few of research works dealing with CF in plants deal with time-domain analysis of the chlorophyll fluorescence dynamics (for a remarkable example, see [60]), and those that do stop short of monitoring long-term processes such as winter dormancy. To the best of our knowledge, this work is the first demonstration of employing a combination of automated data collection across seasons and classic signal processing techniques to achieve data-driven noninvasive assessment of dormancy depth as well as contributions of individual processes affecting PSA during a winter period.

Still there are limitations to overcome. For example, while the suggested approach proved to be suitable for monitoring of dormancy status of plants, prediction of the timing of the onset and release of dormancy would require a more extensive observation across different plant species and climates.

To conclude, our study suggests the use of PAM fluorometry of chlorophyll as a powerful method for probing dormancy phases and stress resilience in plants. Its advantages include scalability and possibility of non-invasive, automated measurements by many remote sensors connected to a computing cloud-based service for collection, analysis, and visualization of the data. As an added benefit, this system could reveal severe damages by frost, which are hard to diagnose visually before the beginning of the warm growing

season. Implementation of such a system at a scale would provide researchers with a tool with unprecedented time resolution and coverage for monitoring dormancy in wild and anthropogenic ecosystems.

For the sake of robustness and to enable the use of time-frequency analysis, it is important to keep the continuous CF record. It is essential for suppressing momentary fluctuations caused by external factors such as weather conditions and other environmental stimuli. Defining of thresholds for detecting the onset or release of dormancy will require additional research. The relevance and efficiency of the developed approach is supported by both destructive measurements and its good agreement with “traditional” chilling requirement models. Moreover, new such models could be developed with relative ease given that an extensive enough CF record is available. Existing models are comparatively coarse and could be further fine-tuned, both for research and practical applications. Obviously, it would not be possible to pinpoint the exact moment of transition between endo- and eco-dormancy since it is unlikely that this transition is momentary. A more confident interpretation of the results of CF-based non-invasive probing of winter dormancy in deciduous plants will require a deeper understanding of the relationship between the phase of their dormancy and the functional state of their PSA.

### Supplementary Materials

*A description of the PAM fluorimeter used in the work, including:*

Figure S1. The key components of laser FRR-fluorimeter.

Figure S2. FRR-technology and synchronous fluorescence detection.

Table S1. JIP-test parameters according to (Strasser et al., 2004 [40])

*Other supplementary figures:*

Figure S3. CF transients measured under dark conditions (at night).

Figure S4. CF transients measured under daylight conditions.

Figure S5. Pearson's  $r$  value matrix computed for pairs of the parameters studied in this work and calculated on the basis of the CF transients measured under daylight conditions.

Figure S6. Pearson's  $r$  value matrix computed for pairs of the parameters studied in this work and calculated on the basis of the CF transients measured under dark conditions (at night).

Figure S7. Autocorrelation plots for select JIP-test parameters and insolation estimates.

Figure S8. Multilinear regression fitted curves for  $F_v/F_m$  and  $DI_0/RC$  using only the meteorological data (ambient temperature and insolation).

*Theoretical background on time series processing, including*

Figure S9. A comparison between Fourier transform and wavelet transform for signal analysis.

**Author Contributions:** Conceptualization, A.S., and B.S.; formal analysis, A.S., and B.S.; data curation, A.S.; investigation, A.S., and I.K.; methodology, A.S., and B.S.; validation, B.S., A.S., S.K., and I.K.; software, B.S., I.K., and S.K.; project administration, supervision, and funding acquisition, A.S.; writing – original draft preparation, A.S. and B.S.; writing – review & editing, B.S., A.S., I.K., and S.K. All authors have read and agreed to the published version of the manuscript.

**Funding:** This work was supported by a grant of the Ministry of Science and Higher Education of the Russian Federation for large scientific projects in priority areas of scientific and technological development (grant number 075-15-2020-774).

**Data Availability Statement:** The raw data and derived parameters are available from the corresponding author on reasonable request.

Code used in the analysis, accompanied with a subset of the data, is available on GitHub (<https://github.com/Lodinn/PAM-timeseries>).

**Acknowledgments:** The indoors chlorophyll fluorescence measurements were carried out at the Phototrophic Organisms Phenotyping user facilities of Lomonosov Moscow State University. The

support from the “Brain, Cognitive Systems, and Artificial intelligence” scientific school of Lomonosov Moscow State University is acknowledged. The authors are deeply thankful to Dr. Alexandr Rappoport (Botanical Garden, MSU) for his invaluable support.

**Conflicts of Interest:** The authors declare no conflict of interest. The funders had no role in the design of the study; in the collection, analyses, or interpretation of data; in the writing of the manuscript; or in the decision to publish the results.

## References

- Withers, P.; Cooper, C. Dormancy. In *Encyclopedia of ecology*, Fath, B.D., Ed. Elsevier: 2018; Vol. 3, pp. 309-314.
- Allona, I.; Ramos, A.; Ibáñez, C.; Contreras, A.; Casado, R.; Aragoncillo, C. Review. Molecular control of winter dormancy establishment in trees. *Spanish Journal of Agricultural Research* **2008**, *6*, 201-210.
- Arora, R.; Rowland, L.J.; Tanino, K. Induction and release of bud dormancy in woody perennials: a science comes of age. *HortScience* **2003**, *38*, 911-921.
- Yu, J.; Conrad, A.O.; Decroocq, V.; Zhebentyayeva, T.; Williams, D.E.; Bennett, D.; Roch, G.; Audergon, J.-M.; Dardick, C.; Liu, Z., et al. Distinctive Gene Expression Patterns Define Endodormancy to Ecodormancy Transition in Apricot and Peach. *Frontiers in Plant Science* **2020**, *11*, doi:10.3389/fpls.2020.00180.
- Considine, M.J.; Considine, J.A. On the language and physiology of dormancy and quiescence in plants. *J Exp Bot* **2016**, *67*, 3189-3203, doi:10.1093/jxb/erw138.
- Rohde, A.; Bhalerao, R.P. Plant dormancy in the perennial context. *Trends Plant Sci* **2007**, *12*, 217-223, doi:10.1016/j.tplants.2007.03.012.
- Campoy, J.A.; Ruiz, D.; Egea, J. Dormancy in temperate fruit trees in a global warming context: A review. *Scientia Horticulturae* **2011**, *130*, 357-372, doi:10.1016/j.scienta.2011.07.011.
- Luedeling, E. Climate change impacts on winter chill for temperate fruit and nut production: A review. *Scientia Horticulturae* **2012**, *144*, 218-229, doi:10.1016/j.scienta.2012.07.011.
- Yamane, H.; Wada, M.; Honda, C.; Matsuura, T.; Ikeda, Y.; Hirayama, T.; Osako, Y.; Gao-Takai, M.; Kojima, M.; Sakakibara, H. Overexpression of Prunus DAM6 inhibits growth, represses bud break competency of dormant buds and delays bud outgrowth in apple plants. *PLoS one* **2019**, *14*, e0214788.
- Maurya, J.P.; Bhalerao, R.P. Photoperiod- and temperature-mediated control of growth cessation and dormancy in trees: a molecular perspective. *Ann Bot* **2017**, *120*, 351-360, doi:10.1093/aob/mcx061.
- Moser, M.; Asquini, E.; Miolli, G.V.; Weigl, K.; Hanke, M.-V.; Flachowsky, H.; Si-Ammour, A. The MADS-Box Gene MdDAM1 Controls Growth Cessation and Bud Dormancy in Apple. *Frontiers in Plant Science* **2020**, *11*, doi:10.3389/fpls.2020.01003.
- Heide, O.M. Interaction of photoperiod and temperature in the control of growth and dormancy of Prunus species. *Scientia Horticulturae* **2008**, *115*, 309-314.
- Cattani, A.M.; Sartor, T.; da Silveira Falavigna, V.; Porto, D.D.; Silveira, C.P.; de Oliveira, P.R.D.; Revers, L.F. The Control of Bud Break and Flowering Time in Plants: Contribution of Epigenetic Mechanisms and Consequences in Agriculture and Breeding. In *Advances in Botanical Research*, Elsevier: **2018**; Vol. 88, pp. 277-325.
- Porto, D.D.; Bruneau, M.; Perini, P.; Anzanello, R.; Renou, J.-P.; Santos, H.P.d.; Fialho, F.B.; Revers, L.F. Transcription profiling of the chilling requirement for bud break in apples: a putative role for FLC-like genes. *Journal of Experimental Botany* **2015**, *66*, 2659-2672.
- Luedeling, E.; Brown, P.H. A global analysis of the comparability of winter chill models for fruit and nut trees. *International Journal of Biometeorology* **2011**, *55*, 411-421.
- Salama, A.-M.; Ezzat, A.; El-Ramady, H.; Alam-Eldein, S.M.; Okba, S.K.; Elmenofy, H.M.; Hassan, I.F.; Illés, A.; Holb, I.J. Temperate fruit trees under climate change: Challenges for dormancy and chilling requirements in warm winter regions. *Horticulturae* **2021**, *7*, 86.
- Erez, A. Bud dormancy; phenomenon, problems and solutions in the tropics and subtropics. In *Temperate fruit crops in warm climates*, Springer: 2000; pp. 17-48.
- Zhang, H.-S.; Li, D.-M.; Tan, Q.-P.; Gao, H.-Y.; Gao, D.-S. Photosynthetic activities, C 3 and C 4 indicative enzymes and the role of photoperiod in dormancy induction in ‘Chunjie’ peach. *Photosynthetica* **2015**, *53*, 269-278.
- Demidchik, V.V.; Shashko, A.Y.; Bandarenka, U.Y.; Smolikova, G.N.; Przhevalskaya, D.A.; Charnysh, M.A.; Pozhvanov, G.A.; Barkosvkiy, A.V.; Smolich, I.I.; Sokolik, A.I., et al. Plant Phenomics: Fundamental Bases, Software and Hardware Platforms, and Machine Learning. *Russian Journal of Plant Physiology* **2020**, *67*, 397-412, doi:10.1134/s1021443720030061.
- McAusland, L.; Atkinson, J.A.; Lawson, T.; Murchie, E.H. High throughput procedure utilising chlorophyll fluorescence imaging to phenotype dynamic photosynthesis and photoprotection in leaves under controlled gaseous conditions. *Plant Methods* **2019**, *15*, 109, doi:10.1186/s13007-019-0485-x.
- Watt, M.; Fiorani, F.; Usadel, B.; Rascher, U.; Muller, O.; Schurr, U. Phenotyping: New Windows into the Plant for Breeders. *Annu Rev Plant Biol* **2020**, *10.1146/annurev-arplant-042916-041124*, doi:10.1146/annurev-arplant-042916-041124.
- Valcke, R. Can chlorophyll fluorescence imaging make the invisible visible? *Photosynthetica* **2021**, *10.32615/ps.2021.017*, doi:10.32615/ps.2021.017.

23. Perez-Bueno, M.L.; Pineda, M.; Baron, M. Phenotyping Plant Responses to Biotic Stress by Chlorophyll Fluorescence Imaging. *Front Plant Sci* **2019**, *10*, 1135, doi:10.3389/fpls.2019.01135.
24. Keller, B.; Matsubara, S.; Rascher, U.; Pieruschka, R.; Steier, A.; Kraska, T.; Muller, O. Genotype Specific Photosynthesis x Environment Interactions Captured by Automated Fluorescence Canopy Scans Over Two Fluctuating Growing Seasons. *Frontiers in Plant Science* **2019**, *10*, doi:10.3389/fpls.2019.01482.
25. Perks, M.P.; Monaghan, S.; O'Reilly, C.; Osborne, B.A.; Mitchell, D.T. Chlorophyll fluorescence characteristics, performance and survival of freshly lifted and cold stored Douglas fir seedlings. *Annals of Forest Science* **2001**, *58*, 225-235.
26. Hawkins, C.; Lister, G. In vivo chlorophyll fluorescence as a possible indicator of the dormancy stage in Douglas-fir seedlings. *Canadian Journal of Forest Research* **1985**, *15*, 607-612, doi:10.1139/x85-099.
27. Alekseev, A.; Matorin, D.; Osipov, V.; Venediktov, P. Investigation of the photosynthetic activity of bark phelloderm of arboreal plants using the fluorescent method. *Moscow University Biological Sciences Bulletin* **2007**, *62*, 164-170.
28. Tikhonov, K.; Khristin, M.; Klimov, V.; Sundireva, M.; Kreslavski, V.; Sidorov, R.; Tsidendambayev, V.; Savchenko, T. Structural and functional characteristics of photosynthetic apparatus of chlorophyll-containing grape vine tissue. *Russian Journal of Plant Physiology* **2017**, *64*, 73-82.
29. Wilson, B.C.; Jacobs, D.F. Chlorophyll fluorescence of stem cambial tissue reflects dormancy development in *Juglans nigra* seedlings. *New Forests* **2012**, *43*, 771-778.
30. Damesin, C. Respiration and photosynthesis characteristics of current-year stems of *Fagus sylvatica*: from the seasonal pattern to an annual balance. *New Phytologist* **2003**, *158*, 465-475.
31. Lennartsson, M.; Ögren, E. Predicting the cold hardiness of willow stems using visible and near-infrared spectra and sugar concentrations. *Trees* **2003**, *17*, 463-470.
32. Öquist, G.; Brunes, L.; Hällgren, J.E.; Gezelius, K.; Hallé, M.; Malmberg, G. Effects of artificial frost hardening and winter stress on net photosynthesis, photosynthetic electron transport and RuBP carboxylase activity in seedlings of *Pinus silvestris*. *Physiologia Plantarum* **1980**, *48*, 526-531.
33. Grebe, S.; Trotta, A.; Bajwa, A.A.; Suorsa, M.; Gollan, P.J.; Jansson, S.; Tikkanen, M.; Aro, E.M. The unique photosynthetic apparatus of Pinaceae - Analysis of photosynthetic complexes in Norway spruce (*Picea abies*). *J Exp Bot* **2019**, 10.1093/jxb/erz127, doi:10.1093/jxb/erz127.
34. Grebe, S.; Trotta, A.; Bajwa, A.; Mancinia, I.; Bag, P.; Jansson, S.; Tikkanen, M.; Aro, E.M. Specific thylakoid protein phosphorylations are prerequisites for overwintering of Norway spruce (*Picea abies*) photosynthesis. *Proceedings of the National Academy of Sciences* **2020**, 10.1073/pnas.2004165117, doi:10.1073/pnas.2004165117.
35. Ivanov, A.; Sane, P.; Zeinalov, Y.; Simidjiev, I.; Huner, N.; Öquist, G. Seasonal responses of photosynthetic electron transport in Scots pine (*Pinus sylvestris* L.) studied by thermoluminescence. *Planta* **2002**, *215*, 457-465.
36. Kalaji, H.M.; Schansker, G.; Brestic, M.; Bussotti, F.; Calatayud, A.; Ferroni, L.; Goltsev, V.; Guidi, L.; Jajoo, A.; Li, P., et al. Frequently asked questions about chlorophyll fluorescence, the sequel. *Photosynth Res* **2017**, *132*, 13-66, doi:10.1007/s11120-016-0318-y.
37. Goltsev, V.N.; Kalaji, H.M.; Paunov, M.; Bąba, W.; Horacek, T.; Mojski, J.; Kociel, H.; Allakhverdiev, S.I. Variable chlorophyll fluorescence and its use for assessing physiological condition of plant photosynthetic apparatus. *Russian Journal of Plant Physiology* **2016**, *63*, 869-893, doi:10.1134/s1021443716050058.
38. Stirbet, A.; Riznichenko, G.Y.; Rubin, A.B.; Govindjee. Modeling chlorophyll a fluorescence transient: Relation to photosynthesis. *Biochemistry Moscow* **2014**, *79*, 291-323, doi:10.1134/s0006297914040014.
39. Maxwell, K.; Johnson, G. Chlorophyll fluorescence-a practical guide. *J Exp Bot* **2000**, *51*, 659-668.
40. Strasser, R.; Tsimilli-Michael, M.; Srivastava, A. Analysis of the chlorophyll a fluorescence transient. In *Chlorophyll a fluorescence: a signature of photosynthesis*, Papageorgiou, G., Govindjee, Eds. Springer: **2004**; pp. 321-362.
41. Linkosalo, T.; Heikkinen, J.; Pulkkinen, P.; Mäkipää, R. Fluorescence measurements show stronger cold inhibition of photosynthetic light reactions in Scots pine compared to Norway spruce as well as during spring compared to autumn. *Frontiers in plant science* **2014**, *5*, 264.
42. Sundblad, L.-G.; Sjöström, M.; Malmberg, G.; Öquist, G. Prediction of frost hardiness in seedlings of Scots pine (*Pinus sylvestris*) using multivariate analysis of chlorophyll a fluorescence and luminescence kinetics. *Canadian Journal of Forest Research* **1990**, *20*, 592-597.
43. Sakar, E.H.; El Yamani, M.; Rharrabti, Y. Frost susceptibility of five almond [*Prunus dulcis* (mill.) DA Webb] cultivars grown in north-eastern Morocco as revealed by chlorophyll fluorescence. *International Journal of Fruit Science* **2017**, *17*, 415-422.
44. Savitch, L.; Leonardos, E.; Krol, M.; Jansson, S.; Grodzinski, B.; Huner, N.; Öquist, G. Two different strategies for light utilization in photosynthesis in relation to growth and cold acclimation. *Plant, Cell & Environment* **2002**, *25*, 761-771.
45. Corcuera, L.; Gil-Pelegrin, E.; Notivol, E. Intraspecific variation in *Pinus pinaster* PSII photochemical efficiency in response to winter stress and freezing temperatures. *PLoS One* **2011**, *6*, e28772.
46. Chang, C.Y.; Brautigam, K.; Huner, N.P.A.; Ensminger, I. Champions of winter survival: cold acclimation and molecular regulation of cold hardiness in evergreen conifers. *New Phytol* **2021**, *229*, 675-691, doi:10.1111/nph.16904.
47. Heide, O.; Prestrud, A. Low temperature, but not photoperiod, controls growth cessation and dormancy induction and release in apple and pear. *Tree physiology* **2005**, *25*, 109-114.

48. Weinberger, J.H. Chilling requirements of peach varieties. In *Proceedings of American Society for Horticultural Science*; **1950**, pp. 122-128.
49. Richardson, E.; Seeley, S.; Walker, D. A model for estimating the completion of rest for "Redhaven" and "Elberta" peach trees. *Hortscience* **1974**, *9*, 331-332.
50. Gilreath, P.; Buchanan, D. Rest prediction model for low-chilling" Sungold" nectarine. *J Am Soc Hortic Sci* **1981**, *106*, 426-429.
51. Shaltout, A.; Unrath, C. Rest completion prediction model for Starkrimson Delicious apples. *Journal of the American Society for Horticultural Science* **1983**, *108*, 957-961.
52. Kolber, Z.S.; Prášil, O.; Falkowski, P.G. Measurements of variable chlorophyll fluorescence using fast repetition rate techniques: defining methodology and experimental protocols. *Biochimica et Biophysica Acta (BBA)-Bioenergetics* **1998**, *1367*, 88-106.
53. Antal, T.; Konyukhov, I.; Volgusheva, A.; Plyusnina, T.; Khruschev, S.; Kukarskikh, G.; Goryachev, S.; Rubin, A. Chlorophyll fluorescence induction and relaxation system for the continuous monitoring of photosynthetic capacity in photobioreactors. *Physiologia plantarum* **2019**, *165*, 476-486.
54. Plyusnina, T.Y.; Khruschev, S.; Degtereva, N.; Konyukhov, I.; Solovchenko, A.; Kouzmanova, M.; Goltsev, V.; Riznichenko, G.; Rubin, A. Gradual changes in the photosynthetic apparatus triggered by nitrogen depletion during microalgae cultivation in photobioreactor. *Photosynthetica* **2020**, *58*, 443-451.
55. Plyusnina, T.Y.; Khruschev, S.; Riznichenko, G.Y.; Rubin, A. An analysis of the chlorophyll fluorescence transient by spectral multi-exponential approximation. *Biophysics* **2015**, *60*, 392-399.
56. Folkner, W.M.; Williams, J.G.; Boggs, D.H.; Park, R.S.; Kuchynka, P. The planetary and lunar ephemerides DE430 and DE431. *Interplanetary Network Progress Report* **2014**, *196*, 42-196.
57. Meinel, A.; Meinel, M. Applied Solar Energy: an Introduction. *NASA STI/Recon Technical Report A*. **1977**, *77*, 33445.
58. Huner, N.; Dahal, K.; Hollis, L.; Bode, R.; Rosso, D.; Krol, M.; Ivanov, A.G. Chloroplast redox imbalance governs phenotypic plasticity: the "grand design of photosynthesis" revisited. *Frontiers in Plant Science* **2012**, *3*, doi:10.3389/fpls.2012.00255.
59. Huner, N.; Öquist, G.; Sarhan, F. Energy balance and acclimation to light and cold. *Trends in plant science* **1998**, *3*, pp. 224-230.
60. Nedbal, L.; Lazár, D. Photosynthesis dynamics and regulation sensed in the frequency domain. *Plant Physiology* **2021**, *187*, pp. 646-661.
61. Heisenberg, W. Über den anschaulichen Inhalt der quantentheoretischen Kinematik und Mechanik. *Zeitschrift für Physik* **1927**, *43*, pp. 172-198.
62. Gabor, D. Theory of communication. *Journal of the Institution of Electrical Engineers* **1946**, *93*, pp. 429-441.
63. Boashash, B. *Time-Frequency Signal Analysis and Processing: A Comprehensive Reference*. Academic Press, London, United Kingdom, 2016; pp. 1-49.
64. Tan, L., Jiang, J. Image filtering enhancement. In: *Digital signal processing: fundamentals and applications*, 3rd ed., Acquisition Editor: Merken, S., Eds.; Publisher: Academic Press London, United Kingdom, 2018; pp. 673-683.